communications biology

Article

https://doi.org/10.1038/s42003-024-07272-5

Age-dependent effects of vaping on the prefrontal cortex, ventral tegmental area, and nucleus accumbens

Check for updates

Brandon J. Henderson ✉, Lauren E. Young, Nathan A. Olszewski, Samuel Tetteh-Quarshie, Sarah K. Maddox, M. Alex Simpkins, Mathew C. Dudich, M. Sage McGlauglin, Zoie C. Weinsweig & Skylar Y. Cooper

Electronic nicotine delivery systems (ENDS) are unique from combustible cigarettes due to the availability of flavor options which make these devices popular among adolescents. However, there are no preclinical investigations into the impact of vaporized nicotine on late-developing brain regions such as the prefrontal cortex. Here, we investigated how neuronal function and drug self-administration differed between adult-exposed and adolescent-exposed mice. Male and female adolescent and adult C57BL/6J mice were used in a 20-session e-Vape® self-administration (EVSA) assay. Brains were then extracted and acute slices were used for either patch-clamp electrophysiology or fast-scan cyclic voltammetry. Adolescent-exposed males exhibited greater reinforcement-related behavior compared to their adult-exposed counterparts. However, adolescent-exposed and adult-exposed females exhibited similar levels of reinforcement-related behavior. Adolescent-exposed mice exhibited significant increases in intrinsic excitability of medial prefrontal cortex (mPFC) pyramidal neurons. Additionally, reinforcement-related behavior observed during EVSA assays correlated with adolescent-exposed mPFC neuronal excitability. This did not occur in adult-exposed mice. In the ventral tegmental area (VTA), we observed that upregulation of nicotinic acetylcholine receptors (nAChRs) only correlated with nicotine self-administration in adult and not adolescent-exposed mice. The relationship between self-administration and changes in neuronal excitability in adolescent mice indicates that the mPFC may be important for adolescent nicotine dependence.

The landscape of nicotine dependence is continuously transforming with the advent of vaping, heralded as a harm reduction strategy among adult cigarette smokers. However, as the rates of combustible cigarette smoking recede among American teens, adolescent vaping has emerged as a new concern[1–3]. While the harm reduction potential for adults transitioning from cigarettes to vaping is acknowledged, the potential risks for vaping-naive individuals, particularly adolescents, are becoming increasingly apparent. Regardless of age, tobacco and nicotine dependence remains a critical public health concern as combustible cigarette use continues to contribute to ~500,000 preventable deaths each year in America alone[4]. While morbidity and mortality risks associated with electronic nicotine delivery systems (ENDS) are still being evaluated, much remains unknown regarding how vaping-related exposure to nicotine alters neurons occupied by nicotinic acetylcholine receptors (nAChRs) in brain regions that impact reward- and reinforcement-related behaviors.

Here, we utilized an e-Vape self-administration (EVSA) assay to examine differences between vaping-related nicotine reinforcement between adult and adolescent mice. ENDS usage is highly correlated with flavor exposure as >95% of adolescent ENDS users and >85% of adult ENDS users exclusively vape with flavors[3,5–7]. We have previously characterized in our mouse models that flavors enhance the self-administration of vaporized nicotine[8,9]. Accordingly, we examined reinforcement-related behavior in adolescent and adult mice using nicotine (6 mg/mL or 60 mg/mL) plus menthol (15 mg/mL). We then utilized these same animals exposed to nicotine in our EVSA assays for patch-clamp electrophysiology, fast-scan cyclic voltammetry, or microscopy assays to examine changes in nicotinic acetylcholine receptor (nAChR) density.

Department of Biomedical Sciences, Joan C Edwards School of Medicine at Marshall University, Huntington, WV, USA. ✉e-mail: Hendersonbr@marshall.edu

Given that the prefrontal cortex is a late-stage developmental brain area[10], we were keen to examine how nicotine-induced changes in the medial prefrontal cortex (mPFC) differed between adults and adolescents. The pathway from the prelimbic (PL)-mPFC to nucleus accumbens core (NAcc) regulates cocaine reinforcement and reinstatement-related behaviors[11]. This pathway has also been identified as a critical pathway in mediating resilience or vulnerability to reinforcement-related behavior to food[12]. Additional investigations have revealed that activity within the mPFC exerts a potential role in the restraint of reward-seeking[13].

Few investigations have focused on the mPFC in the context of nicotine reward and reinforcement using rodent models. Using an adolescent rat model, a previous investigation observed that 3X daily non-contingent administration of nicotine (0.4 mg/kg, subcutaneous) produced an enhancement of baseline firing frequency and number of bursting events in the VTA and mPFC[14]. In adult rats, optogenetic inhibition of dorsal mPFC neurons, and not the ventral mPFC, during cue presentation in an intravenous nicotine self-administration paradigm enhanced nicotine self-administration[15]. Conversely, no enhancements were observed when optogenetic inhibition was delivered after cue presentation. These results suggest that the dorsal mPFC neurons mediate nicotine-associated cues.

In the present study, we investigated the differences between adolescent-exposed and adult-exposed, male and female mice to nicotine vapor self-administration. We investigated changes in the intrinsic excitability of neurons in the mPFC and VTA that occurred as a consequence of nicotine self-administration. We also investigated how age-dependent exposure to nicotine vapor self-administration differentially impacted changes in NAcc dopamine release. Finally, we used fluorescent microscopy to examine age-dependent exposure to nicotine vapor self-administration on nAChR upregulation.

Results

Adolescent-exposed male mice exhibit greater reinforcement-related behavior than adult-exposed male mice to 60 mg/mL nicotine plus menthol

In comparing reinforcement-related behavior with 6 mg/mL or 60 mg/mL nicotine-containing e-liquids, we previously reported that adult male and female mice exhibit different preferences for nicotine doses in our EVSA paradigm[16]. We previously observed that adult male mice exhibited greater reinforcement-related behavior to 6 mg/mL nicotine plus menthol while adult female mice exhibited greater reinforcement-related behavior to 60 mg/mL nicotine plus menthol[16]. Here, we assigned adolescent mice (started at 6–7 weeks old) to e-liquids containing 6 mg/mL nicotine or 60 mg/mL nicotine (both with 15 mg/mL menthol) (Fig. 1, Figs. S1 and S2A1-4). We have previously determined that menthol-alone does not promote reward-related[17] or reinforcement-related[8] behaviors. For this reason, we did not examine mice with a menthol-only control. While mice started EVSA during adolescence, the duration of the paradigm takes them into young adulthood. Accordingly, we label these mice as adolescent-exposed in comparison to our adult-exposed mice. In our EVSA paradigm, we classify mice as acquiring self-administration (passing) by maintaining 3 or more sessions during the FR3 paradigm at an active-to-inactive nosepoke ratio ≥2. In both male and female adolescent-exposed mice, we observed that mice assigned to 6 mg/mL nicotine plus menthol exhibited a 25% and 19% pass rate for females and males, respectively (Fig. S1). Conversely, adolescent-exposed male and female mice assigned 60 mg/mL nicotine plus menthol were observed to have a 55% and a 69% pass rate (Fig. S1) which is consistent with our previous pass rates[8,18]. For both male and female adolescent-exposed mice that 'passed' in the 6 mg/mL nicotine plus menthol condition, active nosepokes and earned e-Vape deliveries were low (<8 active nosepokes, <2 e-Vape deliveries during FR3 sessions, Figure S1C1–4). These responses were similar to adolescent-exposed mice assigned only to cue-light or control (PGVG) conditions (Fig. S2B1-2).

Adolescent-exposed male and female mice that were assigned to 60 mg/mL nicotine plus menthol exhibited a gradual increase in active nosepokes during transitions between FR1, FR2, and FR3 sessions (Figs. 1B1, B3, S3, and S4). Male and female mice in both age groups exhibited a significant increase in nosepokes during the EVSA paradigm (Fig. S4). Only adolescent-exposed female mice exhibited a significant linear increase in eVape deliveries (Fig. S4C3). All 'passed' mice also exhibited active nosepokes and earned e-Vape deliveries that are consistent with our previous investigations (20–30 FR3 active nosepokes, 7–10 earned e-Vape deliveries during FR3 sessions)[8,18,19]. Adult male and female mice exhibited EVSA behaviors that were similar to what we have previously reported[16] (Fig. 1B2, B4). Adult-exposed and adolescent-exposed male and female mice assigned to 60 mg/mL nicotine plus menthol that 'failed' exhibited EVSA behaviors similar to the PGVG-assigned mice (<8 active nosepokes, <2 e-Vape deliveries, Fig. 1C1–4 compared to Fig. S1D1–4). Given that the 'failed' mice exhibited activity that was similar to PGVG-assigned mice, we determined that the failed mice did not exhibit nicotine reinforcement-related behaviors.

In mice that achieved the acquisition criteria, we compared the mean FR3 active nosepokes (sessions 11–15) and mean breakpoint (sessions 16–18) of mice assigned PGVG or nicotine-containing e-liquids (Fig. 2). Both adolescent-exposed and adult-exposed mice assigned to 60 mg/mL nicotine plus menthol exhibited a significant increase in active nosepokes when compared to PGVG-assigned mice ($p < 0.001$, both age groups, Mann–Whitney, Fig. 2A, B). Adolescent-exposed male mice exhibited a 1.8-fold increase in active nosepokes when compared to adult-exposed male mice (Fig. 2A). As with the male mice, adolescent-exposed and adult-exposed female mice exhibited significantly more active nosepokes compared to their PGVG-assigned counterparts ($p < 0.001$, both age groups, Mann–Whitney, Fig. 2C).

In mice that achieved the acquisition criteria, we also compared the mean breakpoint (defined as the mean of the maximum number of nosepokes achieved during the three PR sessions) of adolescent-exposed and adult-exposed male and female mice (Fig. 2B, D). In both adolescent-exposed and adult-exposed male mice, there was a significant difference between the PGVG-assigned males and 60 mg/mL plus menthol-assigned males ($p < 0.001$ and $p = 0.04$ for adolescent-exposed and adult-exposed, respectively, Mann–Whitney U Test, Fig. 2B). In both adolescent-exposed and adult-exposed female mice, there was a significant difference between females assigned PGVG and 60 mg/mL nicotine plus menthol ($p < 0.0001$, both age groups, Mann–Whitney, Fig. 2D). Finally, adult-exposed females had a significantly higher breakpoint when compared to adolescent-exposed females ($p = 0.0002$, Fig. 2D).

To understand differences in neuronal function and changes in nAChR density, every mouse that completed the EVSA paradigms was used in physiological or microscopy assays (described in following sections). Due to the fact that the majority of mice exposed to 6 mg/mL nicotine containing e-liquids failed to acquire self-administration (see Supplemental Material), the subsequent microscopy and physiology assays utilized only the mice that were exposed to 60 mg/mL nicotine plus menthol or control (PGVG) e-liquids.

Adolescent-exposed mPFC pyramidal neurons exhibit higher intrinsic excitability compared to adult-exposed mice

Upon completion of the EVSA paradigm (<30 min after the final session), the brains of the adolescent-exposed and adult-exposed mice were used in physiology and neurobiology assays. We next investigated how EVSA during adolescence impacted neuronal excitability compared to mice exposed during adulthood. In both adult-exposed and adolescent-exposed mice, we isolated brain slices containing the prelimbic area (PL) of the mPFC (Fig. 3A1–3) from α4-Cherry mice. In the PLmPFC, α4* nAChRs are absent on layer V (LV) pyramidal cells, but are present on LIV and LVI pyramidal cells (Fig. 3A1[20],). In both LV and LVI, α4* nAChRs are present on interneurons. Accordingly, we used α4-mCherry fluorescence to identify the LV/LVI border and targeted pyramidal cells negative for α4-mCherry in LV (Fig. 3A2-3). While these LV cells do not contain α4* nAChRs, they contain α7 nAChRs that mediate excitatory stimulation to the NAcc and VTA[20,21]. While the α4* nAChRs present on LV interneurons are subject to

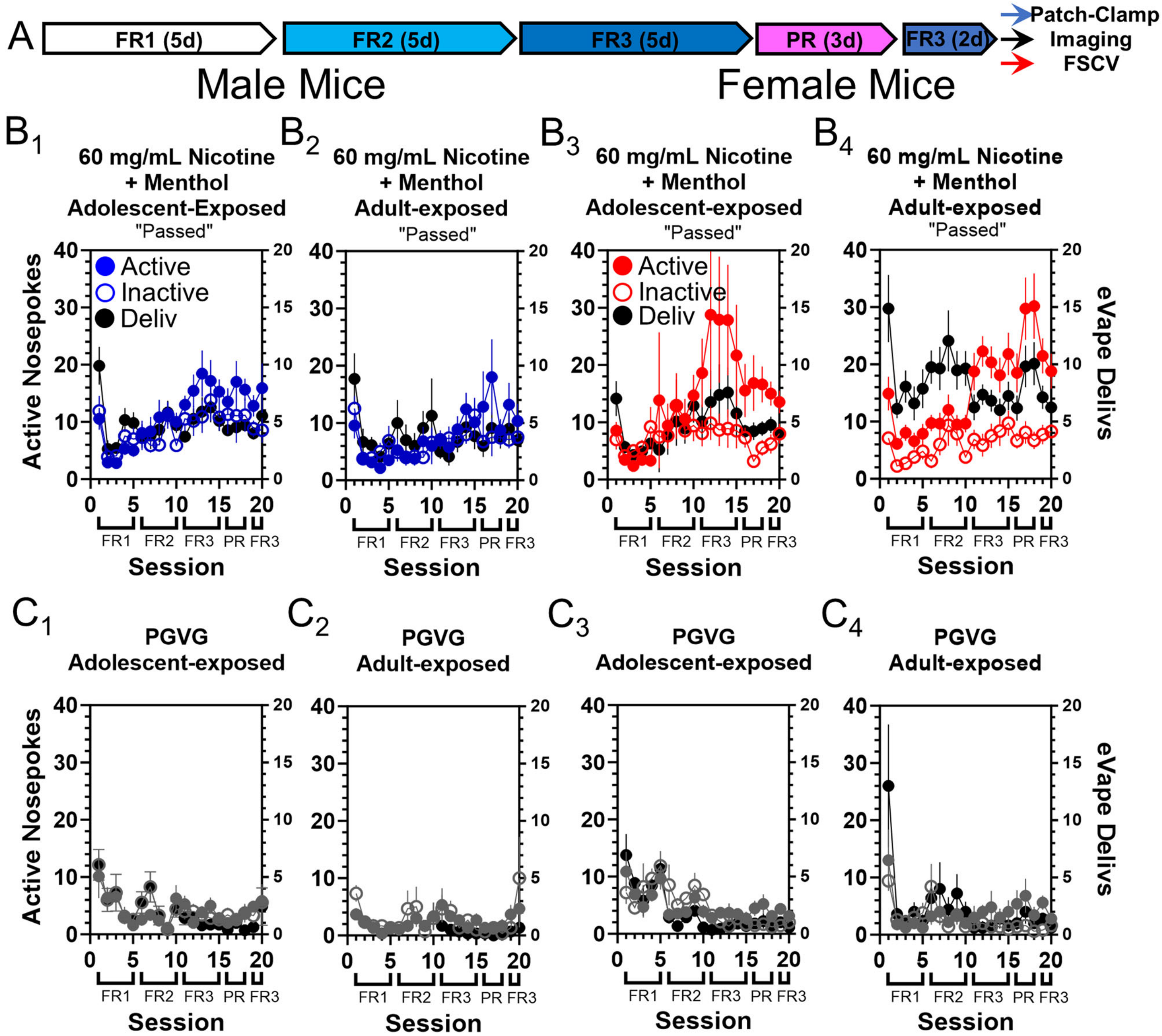

Fig. 1 | Adolescent and adult mouse EVSA with 60 mg/mL nicotine plus menthol. **A** Schematic of EVSA paradigm. $\mathbf{B_{1-4}}$ Active nosepokes (closed red/blue circles), inactive nosepokes (open red/blue circles), and eVape deliveries earned (closed black circles) for adult and adolescent male/female mice during the entire EVSA paradigm that passed acquisition criteria (≥2, active:inactive ratio for ≥3 sessions). $\mathbf{C_{1-4}}$ Adult and adolescent mice assigned to PGVG only. $\mathbf{B_{1-4}}$, $\mathbf{C_{1-4}}$ Right axis shows number of eVape deliveries (black circles). Data are mean ± SEM. For each e-liquid condition and sex, *n* = 16–20 mice per group. Additional control (cue-light only) mice EVSA session data is provided in the supplemental material.

nicotine-induced upregulation and desensitization, we decided to focus on the α7-containing LV pyramidal cells due to their proposed projections to the NAcc and their potential role in modulating dopamine signaling. Using whole-cell patch clamp methods, we used a stepped-current protocol to determine the necessary current to elicit an action potential (rheobase) and the maximum number of spikes during a current step (Fig. 3B1-3, C1-3). We next correlated intrinsic excitability (rheobase) to the mean FR3 active nosepokes of adolescent-exposed and adult-exposed mice (Fig. 3D1-2).

PGVG-assigned mice (mice used in Fig. 1D1-4) exhibited rheobase values between 50 and 80 pA for both adult-exposed and adolescent-exposed male and female mice (Fig. 1D1-2). Therefore, control mice did not exhibit any differences between adult-exposed and adolescent-exposed groups.

In adolescent-exposed male and female mice, we observed that intrinsic excitability increased (rheobase decreased) as mice self-administered more (increased FR3 score, Fig. 3C1). As a decrease in rheobase infers an increase in intrinsic excitability, this suggests that adolescent mice that self-administered more exhibited an increase in excitability of mPFC pyramidal cells ($r^2 = 0.38$, $p = 0.009$, $F_{(1,17)} = 8.7$, Fig. 3D1). In adult-exposed male and female mice, we failed to observe any correlation between mPFC intrinsic excitability and reinforcement-related behavior ($r^2 = 0.11$, $p = 0.21$, $F_{(1,14)} = 1.7$, Fig. 3D2). In adolescent-exposed male and female mice, we also observed that intrinsic excitability increased (rheobase decreased) as mice exhibited an increase in breakpoint ($r^2 = 0.34$, $p = 0.008$, $F_{(1,17)} = 8.9$, Fig. 3E1). We did not observe an association between intrinsic excitability of mPFC neurons and breakpoint in adult-exposed mice ($r^2 = 0.03$, $p = 0.49$, $F_{(1,14)} = 0.49$, Fig. 3E2).

We did not observe a significant difference in the current-voltage relationship between adolescent-exposed and adult-exposed male mice (Fig. S5). However, we observed a significant difference in adolescent-exposed and adult-exposed female mice (mixed effects two-way ANOVA, $F_{(18, 304)} = 6.47$, $p < 0.0001$ and $F_{(1, 209)} = 5.83$, $p = 0.017$ for current-step and age factors, respectively, Fig. S5C2).

Together, these data agree with previous reports that adolescent-exposed mice exhibit enhancements in mPFC neuronal excitability[14].

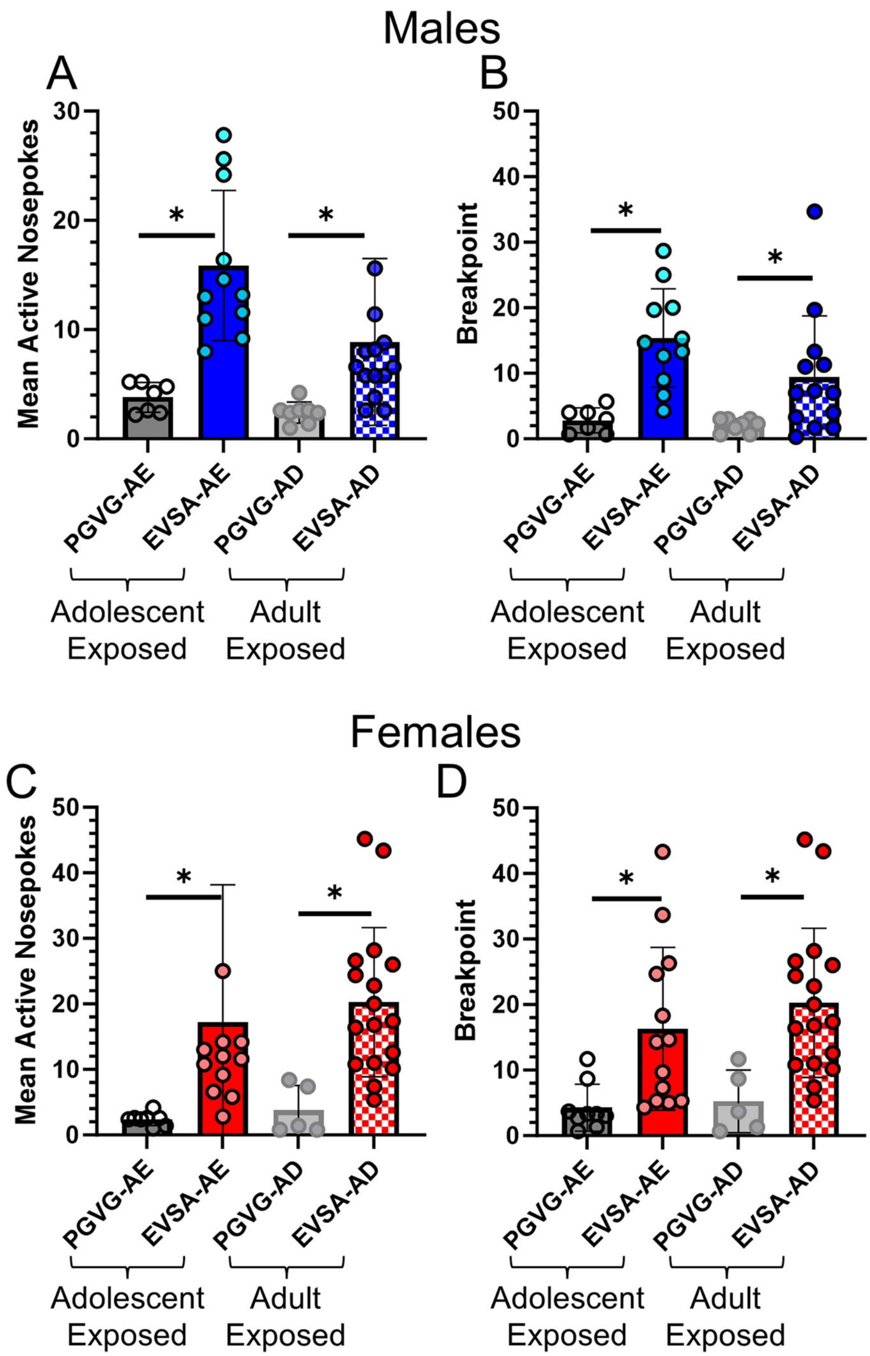

Fig. 2 | Means comparison of FR3 active nosepokes and breakpoint for adult and adolescent mice that pass acquisition criteria. **A**, **B** Mean FR3 active nosepokes and breakpoint for male adult and adolescent mice. **C**, **D** Mean FR3 active nosepokes and breakpoint for female adult and adolescent mice. Data are mean ± SEM. Data are analyzed by a Mann–Whitney U Test. *$p < 0.05$; ****$p < 0.0001$. For each condition, $n = 8$–14. Individual dots in each bar indicate individual mice.

Adolescent-exposed mice exhibit an enhancement in intrinsic excitability and this correlates with the amount of nicotine (plus menthol) self-administered during the EVSA paradigm.

Adolescent-exposed mice exhibit enhancements in VTA dopamine neuron intrinsic excitability

We have previously reported that adult-exposed mice do not exhibit a change in the intrinsic excitability of VTA dopamine neurons that is linked to vapor self-administration behavior[22]. That is, VTA dopamine neuron intrinsic excitability remains relatively unchanged in adult-exposed animals, despite high levels of nicotine intake. Instead, we observed that adult-exposed mice exhibit a correlation between nicotine intake and active:inactive nosepoke distinction[22]. Similar to assays focused on the mPFC, we isolated brain sections that contain the VTA at the completion of EVSA assays (Fig. 4A1-4). We used the presence of α6-GFP to identify putative dopamine neurons in the VTA, similar to our established methods[22–24]. In the VTA, α6 nAChRs are only present on dopamine cells, and they exhibit a > 98% overlap with tyrosine hydroxylase[24]. Because we have previously established that adult-exposed mice do not exhibit changes in VTA dopamine neuron excitability following EVSA assays, we examined only adolescent-exposed mice here. Similar to our investigation into mPFC neuronal excitability, we used a current-step protocol to measure intrinsic excitability (Fig. 4B1-3 and C1-3). We observed that PGVG-assigned mice exhibit rheobase between 40 and 70 pA (Fig. 4D1-2). In adolescent-exposed mice, we observed a significant correlation between rheobase and FR3 score (Fig. 4D1, $r^2 = 0.68$, $p = 0.0003$, $F^{(1,12)} = 25.3$) and mean breakpoint (Fig. 4D2, $r^2 = 0.59$, $p = 0.001$, $F_{(1,12)} = 17.0$). We did not observe a correlation between the maximum number of spikes during current steps and EVSA behaviors (Fig. 4E1-2). Prior investigations have observed that adolescent-exposed rats exhibited an increase in the firing frequency and bursting of VTA neurons[14]. While our observations on enhancements of intrinsic excitability partially agree with this previous report, the different

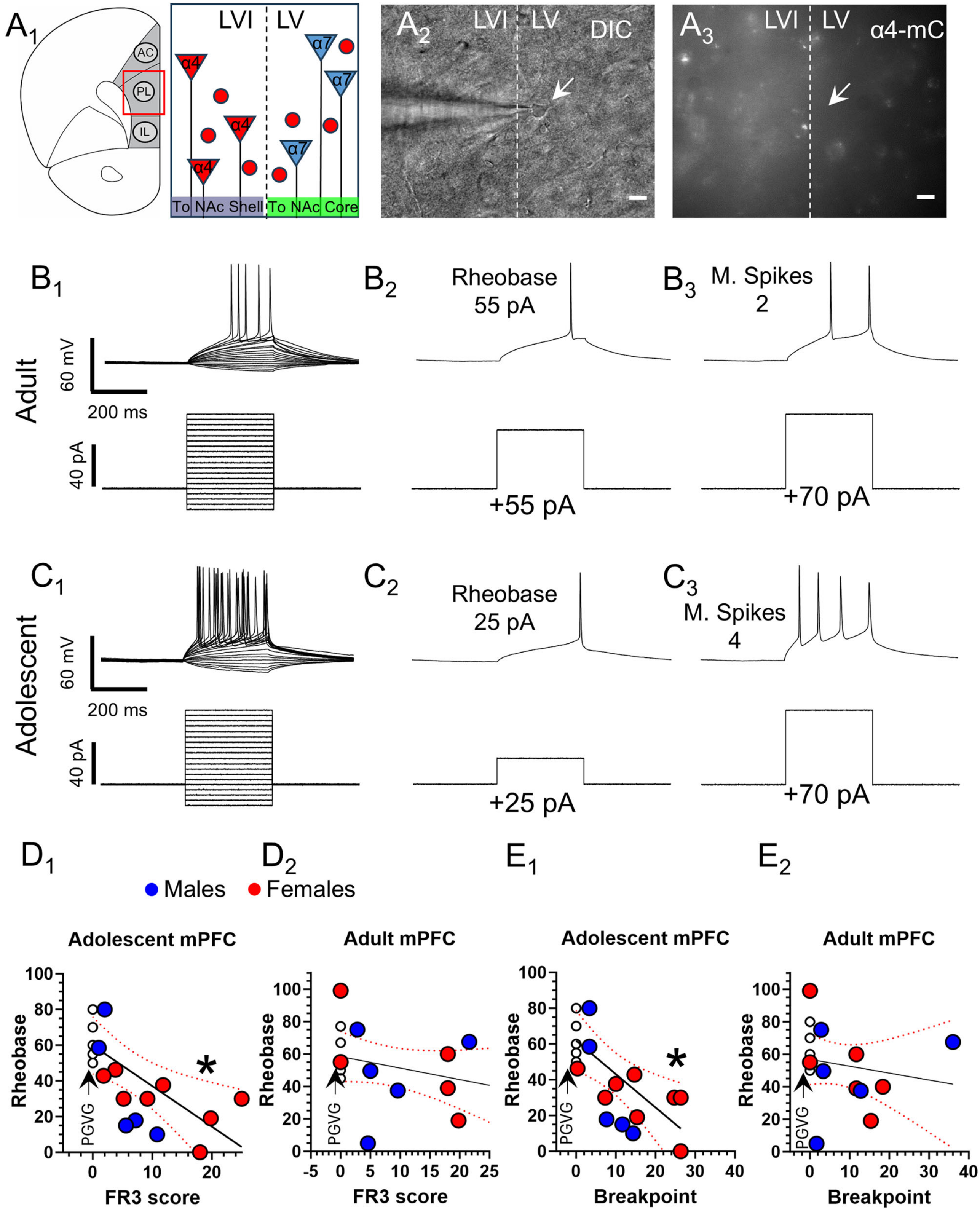

Fig. 3 | Adolescent-exposed mice exhibit enhanced intrinsic excitability in the mPFC. A Representative image of a putative pyramidal neuron in the mPFC PL region in DIC imaging mode (A_2), mCherry fluorescent signal (A_3), and a representative schematic of the target brain area (A_1). $B_{1\text{-}3}$, $C_{1\text{-}3}$ Representative current-clamp waveforms from mPFC pyramidal neurons recorded from adult-exposed and adolescent-exposed mice. $D_{1\text{-}2}$ Correlation of EVSA FR3 score to rheobase of individual adolescent-exposed (D_1) or adult-exposed (D_2) mice. $E_{1\text{-}2}$ Correlation of EVSA breakpoint to rheobase of individual adolescent-exposed (E_1) or adult-exposed (E_2) mice. For $D_{1\text{–}2}$ and $E_{1\text{–}2}$, individual dots represent the mean of rheobase values for individual mice (mean of 2–3 neurons for each mouse. ($D_{1\text{–}2}$, $E_{1\text{–}2}$) For each comparison, n = 14–18 mice. Blue and red data indicate male and female mice, respectively, and open circles indicate mice assigned to control (PGVG). $A_{2\text{–}3}$, bars are 15 µm.

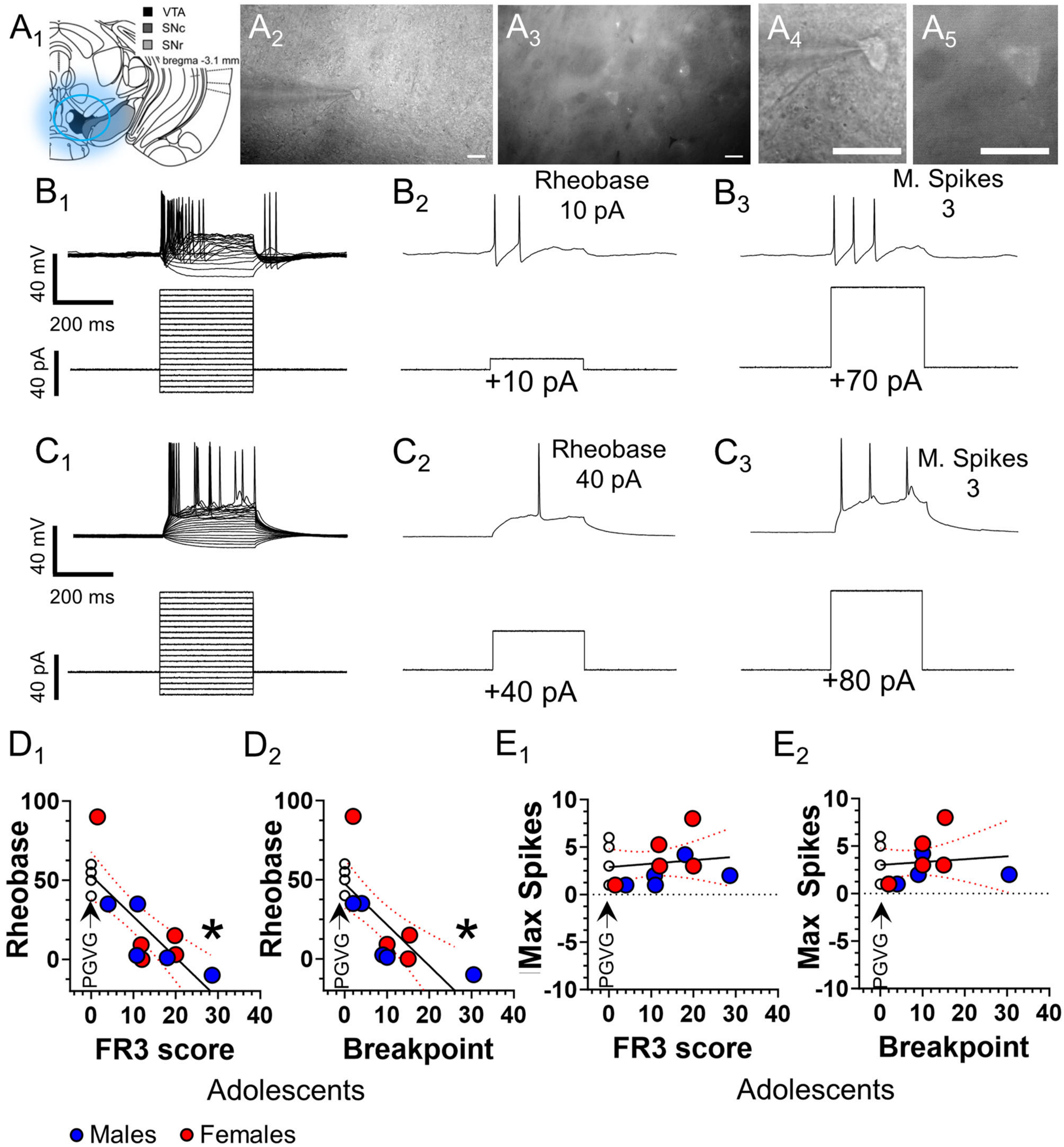

Fig. 4 | Adolescent-exposed mice exhibit enhanced intrinsic excitability in VTA dopamine neurons. $\mathbf{A_1}$ Representative schematic of target brain region (~bregma, -3.3). $\mathbf{A_{2-5}}$ Representative DIC and GFP image of target VTA dopamine neurons imaged on an electrophysiology setup. $\mathbf{B_{1-3}}$, $\mathbf{C_{1-3}}$ Representative waveforms from current-voltage protocols of neurons with different levels of intrinsic excitability. Correlation of EVSA FR3 score to rheobase ($\mathbf{D_1}$) or mean breakpoint ($\mathbf{D_2}$) of individual adolescent-exposed mice. $\mathbf{E_{1-2}}$ Correlation of maximum spikes during a current step to mean FR3 score (E1) or mean breakpoint (**I**). Correlation of baseline firing frequency to mean FR3 score (**J**) or mean breakpoint (**K**). $\mathbf{A_{2-5}}$ Bars, 20 µm. $\mathbf{D_{1-2}}$, $\mathbf{E_{1-2}}$ For each comparison, $n = 14$ mice. Open circles indicate mice assigned to control (PGVG), blue and red data are male and female mice, respectively.

observations may be the result of electrophysiological methods: slice physiology (present study) compared to in vivo recordings[14]. These data indicate that mice exposed to nicotine EVSA during adolescence result in an enhancement in the intrinsic excitability of VTA dopamine neurons.

While our electrophysiological investigations thus far have focused only on mice that passed our EVSA acquisition criteria, we also completed electrophysiological assays in adolescent-exposed mice that failed to reach the 2:1 criteria (Fig. S6). In brain slices containing the VTA or mPFC, we failed to observe an association between FR3 score and intrinsic excitability (rheobase and max spikes) (Fig. S6).

Adolescent-exposed mice exhibit enhanced dopamine release compared to adults

Similar to the electrophysiological assays, brain slices were obtained from mice that completed EVSA assays. Here, slices containing the nucleus accumbens core (NAcc) were utilized in fast-scan cyclic voltammetry

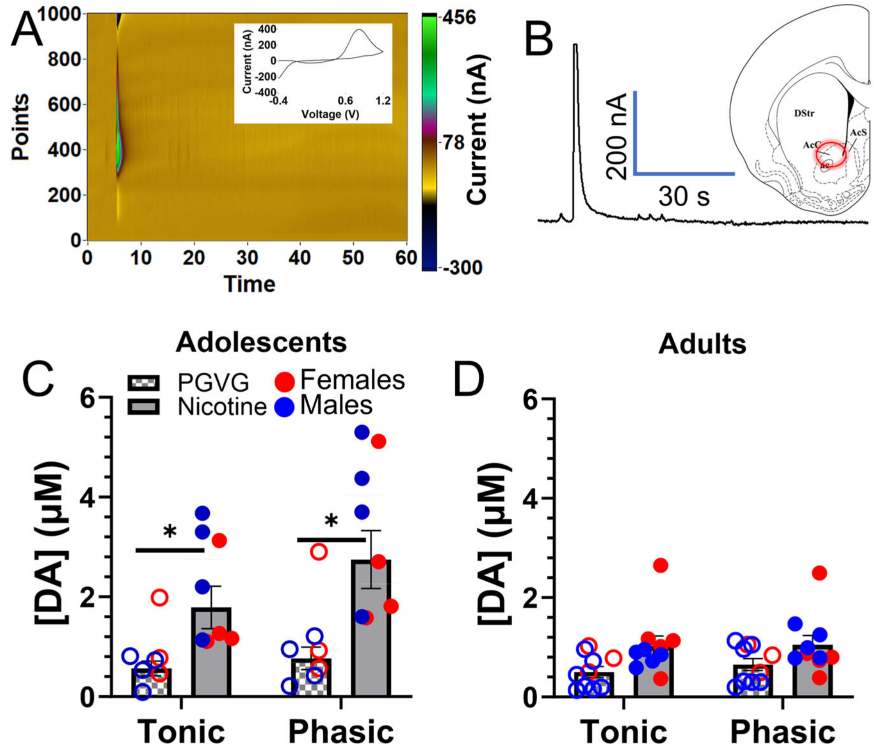

Fig. 5 | Adolescent-exposed mice exhibit enhanced baseline tonic dopamine release in the NAc core. **A** Representative color plot and voltammogram of a phasic (5-pulse, 60 Hz) stimulation in the NAc core. **B** Representative dopamine waveform from a phasic stimulation. **C** Mean tonic-stimulated dopamine release in adolescent-exposed mice from PGVG or nicotine (EVSA) treatment groups. **D** Mean phasic-stimulated dopamine release in adult mice from PGVG or nicotine (EVSA) treatment groups. In (**C**, **D**), data were analyzed by a Mann–Whitney U Test. For each comparison, $n = 5$–10 mice. Data are mean ± SEM. Blue and red data are for males and females, respectively.

(FSCV) assays. Dopamine release was elicited by electrical stimulation that mimicked tonic (5 pulses at 5 Hz) or phasic (5 pulses at 60 Hz) signaling (Fig. 5A, B). In previous investigations, nicotine exposure produced a decrease in tonic-stimulated dopamine release and an increase in phasic-stimulated dopamine release[25]. Using vaporized 6 mg/mL nicotine (without and with menthol), we observed a similar trend in which nicotine exposure decreased tonic-stimulated dopamine release and enhanced phasic-stimulated release[19]. Here, adult-exposed mice that completed the EVSA paradigm with 60 mg/mL nicotine plus menthol exhibited a different trend as both tonic and phasic stimulation produced a non-significant increase in dopamine (Fig. 5D). Regarding adolescent male and female mice, we observed that both tonic and phasic stimulation produced an increase in dopamine release among mice exposed to 60 mg/mL nicotine plus menthol when compared to PGVG ($p = 0.04$ and 0.03 for tonic and phasic, respectively, Mann–Whitney, Fig. 5C). These data suggest that adult mice exposed to high nicotine exhibit little change in electrically stimulated dopamine release in the NAcc. However, adolescent-exposed mice exhibit an enhancement in dopamine release regardless of the stimulation frequency.

Adolescent-exposed mice exhibit lower susceptibility to nAChR upregulation at high nicotine doses

Just as we did with the previously described physiology assays, we extracted brains from mice that completed EVSA assays (Figs. 1 and 2), but here we applied them in fluorescence microscopy assays. We previously established that menthol enhances nicotine-induced upregulation of nAChRs[17] and that nAChR upregulation on VTA dopamine neurons correlates to reward-related behavior[24]. Using similar methods, we used brains from α4mCherryα6GFP mice that completed EVSA assays with 60 mg/mL nicotine and 15 mg/mL menthol in nAChR upregulation assays. We correlated the mean raw integrated density (RID) of nAChR subtypes to reinforcement-related behavior (mean FR3 active nosepokes). In adult mice, we observed a significant correlation for α4* and α4α6* nAChRs ($p = 0.021$ and 0.024, respectively) for reinforcement-related but not mean breakpoint (Fig. 6C, D, G, H, K, L). Thus, mice that exhibited more active nosepokes for vapor delivery exhibited an increase in nAChR density. However, we did not observe any change in nAChR density in adolescent-exposed mice that correlated with EVSA-related behaviors (Fig. 6E, F, I, J, M, N).

Next, we investigated changes in VTA GABA neurons. While α6-GFP overlaps with tyrosine hydroxylase, cells that are GFP(-) but α4-mCherry(+) are likely VTA GABA neurons[26]. Thus, VTA cells that are GFP(-) but mCherry(+) were identified as putative GABA neurons (Fig. 7A). While upregulation was not observed on VTA dopamine neurons in adolescent-exposed mice, we did observe that α4* nAChR upregulation on VTA GABA neurons exhibited a significant positive correlation with FR3 score ($r^2 = 0.38$, $p = 0.045$, Fig. 7D) and breakpoint ($r^2 = 0.60$, $p = 0.0053$, Fig. 7E). Similarly, adult-exposed mice exhibited a significant correlation between α4* nAChR upregulation and FR3 nosepokes ($r^2 = 0.75$, $p = 0.0027$, Fig. 7B) and breakpoint ($r^2 = 0.78$, $p = 0.0016$, Fig. 7C).

EVSA acquisition is dependent upon association with the area close to the vapor port

Finally, we examined what may contribute to why mice may succeed or fail to acquire a 2:1 active:inactive ratio. In a separate cohort of mice, session 15 (final FR3 session) was recorded and the self-administration area was divided into the vapor port zone (VZ) or nosepoke zone (NZ) (Fig. S6A1-2, S6B1-2). We observed mice that passed spent significantly more time in the VZ (Fig. S6C) while mice that failed spent significantly more time in the NZ. We also observed that mice that passed exhibited cotinine plasma values > 60 ng/mL while mice that failed exhibited cotinine values < 40 ng/mL (Fig. S6D1-2). This suggests that failed mice may not actively inhale the vaporized nicotine or are not able to reach high plasma values due to their location in the chamber.

Discussion

Several key criteria need to be met for self-administration paradigms to be translationally relevant to human behavior. EVSA remains a new technique in its infancy. We have consistently shown that mice will escalate their active nosepokes for vaporized nicotine over time in EVSA paradigms (Fig. 1[8,9,16,18]). We have also demonstrated that nAChR antagonists (2 mg/kg DhβE) can block nicotine EVSA[8]. Further, we have shown that mice exhibit extinction-related bursts when transitioned to PGVG[9,23]. Finally, we have also shown that mice will re-acquire self-administration when active and inactive nosepokes are switched[8]. Primarily, this work has been completed with adult mice, however, this present study highlights observed differences

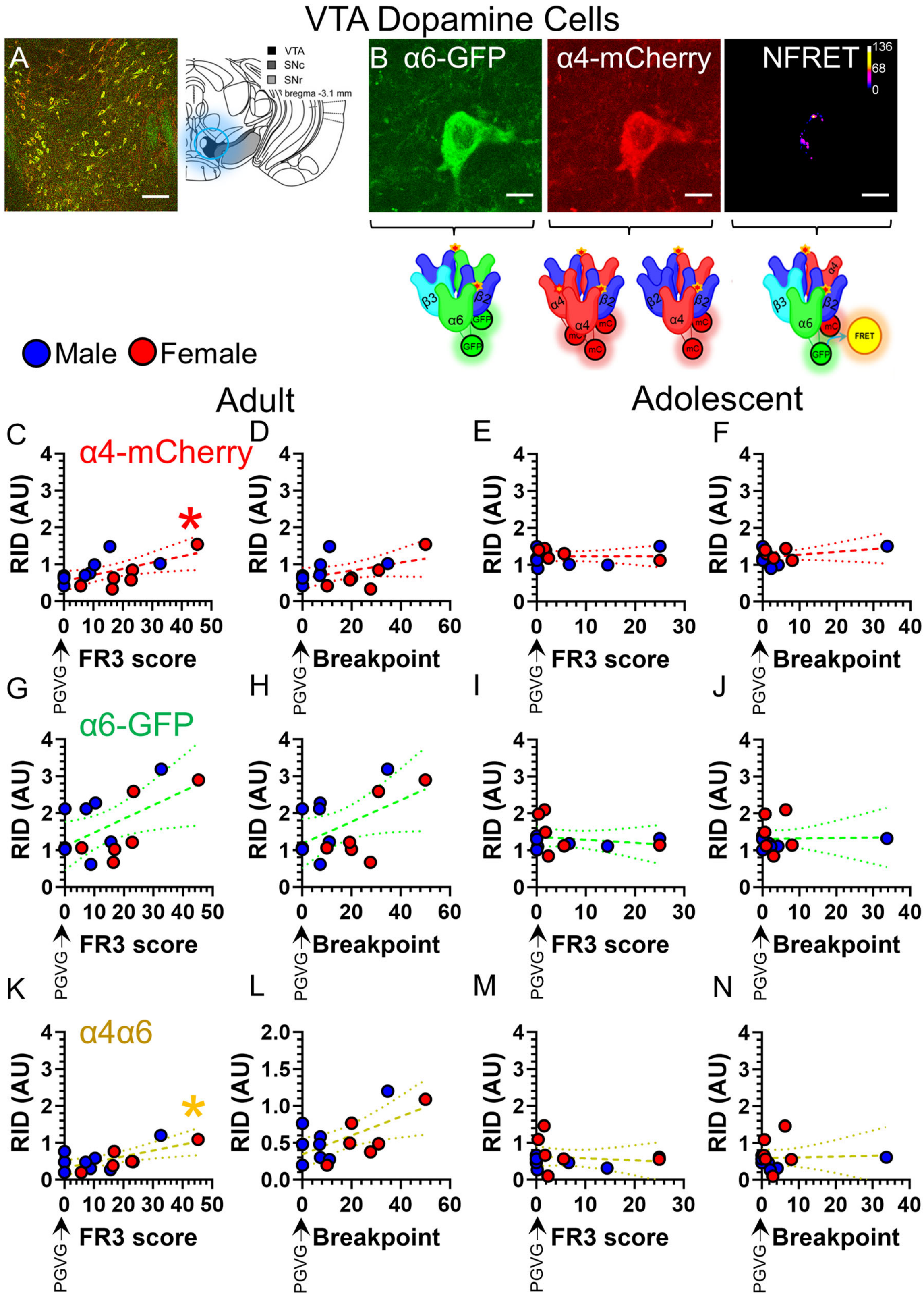

Fig. 6 | Adult-exposed and adolescent-exposed mice exhibit differences in nicotine-induced nAChR upregulation. **A** Representative schematic and 10X image of target VTA region in α4-mCherryα6-GFP mice. **B** Representative 20X (with 10X digital zoom) images of α6-GFP and α4-mCherry fluorescence signals in the VTA of α4-mCherryα6-GFP mice. **C**–**N** Linear regression data for VTA dopamine neuron nAChR RID of adult-exposed and adolescent-exposed mice in relation to FR3 score and breakpoint (mean of maximum active nosepokes during PR sessions). For each condition, $n = 13$–14 mice. Scale bar, 10 µm (**B**) and 100 µm (**A**). Correlations with "*" represent significance ($p < 0.05$). Colored blue and red circles are for male and female mice, respectively.

Fig. 7 | Both adolescent-exposed and adult-exposed mice exhibit upregulation in VTA GABA neurons. **A** Representative 20X (with 10X digital zoom) image of GABA and dopamine cells in the VTA. **B–E** Linear correlation of VTA GABA neuron nAChR RID with FR3 score or PR score for adult-exposed and adolescent-exposed mice. For each condition, $n = 8–11$ mice. Scale bar, 10 µm (**A**). Correlations with "*" represent significance ($p < 0.05$). Blue and red circles are for male and female mice, respectively.

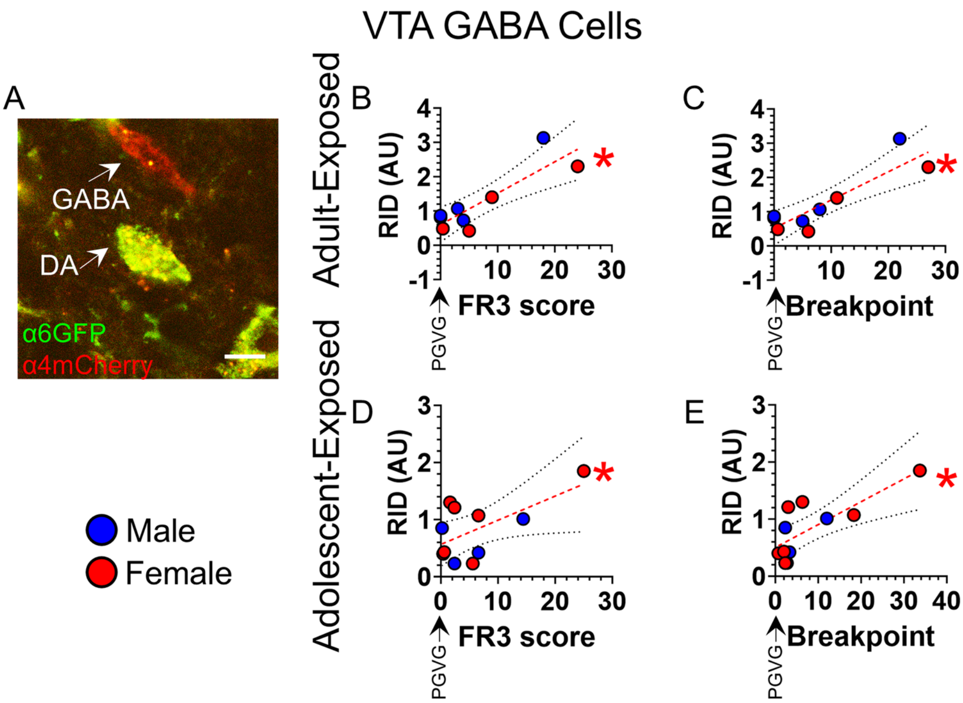

between adolescent-exposed and adult-exposed mice. While the adolescent mice used in this study started at 6–7 weeks of age, the EVSA paradigm was completed when the mice reached adulthood (~10–11 weeks old). For this reason, we use the terms adolescent-exposed and adult-exposed to define the differences in age grouping.

In recent years, increasing adolescent e-cigarette use has sparked concerns about the potential long-term consequences on brain development and susceptibility to nicotine dependence. Building on previous findings that indicated sex-dependent nicotine preferences in adult mice[16], our preclinical investigation focused on physiological changes associated with adolescent vapor self-administration. Specifically, we focused on late-developing brain regions, such as the mPFC, and the VTA due to prior investigations of early nicotine exposure producing a hyper-dopaminergic state[27].

Our study revealed a divergence from previous observations in adult-exposed mice regarding nicotine dose preferences. Both adolescent-exposed males and females exhibited a preference for high doses of nicotine (60 mg/mL) (Fig. 1, Figure S1) despite having previously observed that adult male mice prefer lower (6 mg/mL) doses of nicotine while adult females preferred higher (60 mg/mL doses of nicotine)[16]. Adolescent-exposed male mice exhibited significantly greater reinforcement-related behavior when compared to adult-exposed male mice. However, we did not see a difference between breakpoint of adolescent-exposed or adult-exposed male mice. In female mice, we did not see a difference in reinforcement-related behaviors, but we did observe that adult-exposed female mice exhibited a greater breakpoint when compared to adolescent-exposed female mice.

Notably, we observed heightened intrinsic excitability in prelimbic area mPFC pyramidal cells in adolescent-exposed mice compared to adults (Fig. 3). Strikingly, while self-administration correlated with intrinsic excitability in adolescent-exposed mice, no such relationship was observed in adult-exposed mice. This intriguing finding suggests a potentially distinct mechanism by which nicotine influences the excitability of pyramidal cells during adolescence, possibly playing a critical role in shaping neural circuits involved in nicotine-related reward. Similar to a recent study[28], we found that adolescent and adult mice exhibited similar plasma cotinine values (Fig. S7D1). Thus, we can conclude that differences we observed between adults and adolescents are not due to differences in plasma nicotine/cotinine values.

One potential confound is that many of our measurements occur when our adolescent-exposed mice reach early adulthood. However, this may also provide pertinent information in regards to what physiological changes may persist into adulthood. Previous studies have shown that other drugs of dependence (amphetamine and cocaine) given at adolescent timepoints produce an enhancement in mPFC neuronal excitability by attenuating GABAergic inhibitory signaling and this persists into adulthood[29,30]. We have not examined changes in mPFC GABAergic neurons and this will be a target of follow-up studies. However, given that nicotine has been characterized to attenuate GABAergic signaling through nicotine-induced desensitization[31–33], this is a strong possibility. These data also may suggest a potential consequence of early exposure to vaporized nicotine. Neuroimaging has reinforced the understanding that the PFC not only plays a role in compulsive drug taking but also may account for the negative behaviors associated with addiction and "the erosion of free will"[34]. Early exposure to drugs of dependence increase the risk of lifelong drug dependence[35] and prior reports suggest that early exposure to drugs, and resulting changes in the mPFC, enhance reactivity to cues and sensitivity to reward in adulthood[35]. The changes we observed may be a component of this mechanism, and this will be an additional focus for follow-up investigations.

Another notable distinction between adolescents and adults emerged in the area of VTA dopamine neuron intrinsic excitability and NAcc dopamine release. We previously observed that adult-exposed mice did not exhibit changes in VTA dopamine neuron excitability following nicotine EVSA, but instead we observed that VTA dopamine neuron excitability in adult mice correlated with active-inactive distinction[22]. Here, we observed that adolescent-exposed mice did exhibit a significant correlation with nicotine reinforcement-related behaviors and VTA dopamine neuron intrinsic excitability (Fig. 4). This also partially agrees with a prior investigation into adolescent-exposed mice that utilized in vivo electrophysiological recordings[14]. As we have seen in previous reports[19], mice exposed to our EVSA paradigm exhibited a decrease in tonic-stimulated dopamine release but an increase in phasic-stimulated dopamine release. This is in agreement with previous reports that used FSCV and coronal slices[25]. We must be clear that the results were not statistically significant, but they exhibited a trend consistent with these prior reports. It is possible that adult mice may be more sensitive to changes in 'lower' nicotine concentrations as our previous report used 6 mg/mL nicotine and 6 mg/mL nicotine plus menthol[19]. In adolescent mice, we observed an increase in both tonic-stimulated and phasic-stimulated dopamine release in mice exposed to the EVSA paradigm. The differential regulation of tonic/phasic stimulation by nicotine is in part a consequence of nAChR desensitization and due to the shift toward a higher population of high-sensitivity α4β2 nAChRs[36]. Given we observed that adolescent mice did not exhibit an increase in nAChR density on VTA dopamine neurons with nicotine EVSA exposure, this suggests that the divergence from previous observations is due to the nAChR pool on dopamine neurons being relatively unchanged. Seeing as adolescent mice exhibit an increase in mPFC intrinsic excitability linked to EVSA behaviors, excitatory inputs from the mPFC to the NAc core may play a role in the observed nicotine-induced enhancement of dopamine release.

Adult-exposed mice did not exhibit changes in dopamine release following nicotine exposure, contrasting sharply with enhanced release observed in adolescent-exposed mice. The heightened sensitivity to nicotine-induced enhancements in dopamine release during adolescence raises questions about the neurobiological underpinnings of increased vulnerability to addiction-related behaviors during this critical developmental period.

As discussed above, in adolescent-exposed mice we did not observe nAChR upregulation on VTA dopamine neurons but did on VTA GABA neurons. Previous reports have detailed that nAChRs on VTA dopamine neurons exhibit little to no upregulation[26]. However, additional studies using similar experimental models revealed that this may be concentration-specific[17]. The fact that upregulation did occur on VTA dopamine neurons in adult-exposed mice suggests that upregulation in this region may be concentration- and age-dependent. Regardless, this highlights that additional attention needs to be dedicated toward the examination of nAChR trafficking and its alteration by nicotine (with flavorants) at different developmental stages.

There are several additional confounds that need to be considered. First, our vapor self-administration assay is essentially a whole-body exposure paradigm. While mice inhale vaporized e-liquids there is also the potential for mice to absorb vaping chemicals on their fur which could then contribute to additional exposure during grooming. Second, there is also the case for animal-to-animal variability. While vapor delivery is contingent upon active nosepoke activity, the mice also have their own agency as to where they are positioned when the vapor is delivered to the chamber. This is a key difference to intravenous self-administration paradigms. We believe our separation of passed and failed mice help to control animal-to-animal variability (see Fig. S7D1-2).

In conclusion, our preclinical investigation uncovered unique neurobiological changes in adolescent-exposed mice following vapor self-administration of nicotine. The divergence from adult responses emphasizes the importance of considering developmental stages when studying the effects of nicotine exposure. The heightened intrinsic excitability, altered dopamine release, and nuanced nAChR dynamics observed in adolescent-exposed mice underscore the need for further exploration to elucidate the specific mechanisms that contribute to susceptibility to nicotine dependence during this critical developmental window. As the landscape of e-cigarette use among adolescents continues to evolve, our findings contribute valuable insights that may inform preventive and therapeutic strategies to mitigate the potential long-term consequences of early nicotine exposure. The heightened excitability observed in the medial prefrontal cortex and the altered dopamine release dynamics in key reward-related areas suggest that early exposure to nicotine may have enduring effects on neural circuits that are crucial for decision-making and reward processing. These data emphasize the need for a nuanced understanding of harm reduction strategies. While vaping may offer benefits for adults seeking alternatives to cigarettes, the unique vulnerabilities of the adolescent brain underscore the importance of tailored public health interventions. These findings contribute to a growing body of knowledge that informs regulatory measures and public health initiatives aimed at mitigating the potential risks associated with adolescent vaping.

Material and methods

Mice

All experiments were conducted in accordance with the guidelines for care and use of animals provided by the National Institutes of Health and approved by the Institutional Animal Care and Use Committee at Marshall University. We have complied with all relevant ethical regulations for animal use/ Mice were group housed on a standard 12/12-h light/dark cycle at 22 °C and given food and water *ad libitum*. We used α4-mCherryα6-GFP or α4-mCherry mice (C57BL/6J strain, see ref. 17). These mice are deposited at the Mutant Mouse Resource & Research Centers and are available for general use (MMRRC 068051-MU). Fluorescent nAChR reporter mice have been characterized to exhibit similar nAChR properties when compared to WT C57BL/6J mice[26,37]. Furthermore, these fluorescent nAChRs exhibit pharmacological properties that are similar to their non-fluorescent nAChR counterparts[38,39].

All mice were adolescents (6–7 weeks old) or adults (3-months-old) at the time of starting EVSA assays. Both male and female mice were used and numbers of each are detailed below in the methods for specific experiments and given in detail in corresponding figures.

Drugs and E-liquid composition

Nicotine salt (ditartrate dihydrate) was obtained from Acros Organics (AC415660500). (-)-menthol was obtained from Alfa Aesar (A10474). Propylene glycol was obtained from Tedia (PR1494-065), and vegetable glycerin was obtained from J.T. Baker (2143-01). All e-liquids were mixed with the vehicle, propylene glycol and vegetable glycerin (PGVG; 50:50 ratio), at a final concentration of 15 mg/mL for menthol and 6 mg/mL or 60 mg/mL nicotine. As with our previous studies, the dose of nicotine is respective of nicotine freebase[9,22,23]. Dopamine (dopamine HCL) was obtained from Alfa Aesar (Product #A11136) and used to calibrate FSCV electrodes.

E-Vape® Self-Administration (EVSA) assays

We used a commercial vapor self-administration setup (La Jolla Alcohol Research Inc. (LJARI), La Jolla, CA, USA; www.ljari.tech)[8,9]. Two standard Med-Associates nosepokes (containing yellow cue lights) were mounted above the floor on the back-side walls of the chamber. All chambers were housed in a dark Plexiglas enclosure that minimized extraneous light and noise (operant chambers in one enclosure and passive chambers in another). Airflow was vacuum-controlled by an electric pump that allowed airflow at 1 L/min. E-liquid solutions were contained in Geek Vape® atomizer tanks (0.40Ω dual coil; purchased from LJARI) that were activated by a custom e-cigarette mod box (LJARI, La Jolla, CA, USA). Vapor delivery settings were controlled by an e-Vape® custom controller at 400 °F and 65 W (LJARI, La Jolla, CA, USA). At the end of each 2 h EVSA session, the interior of the chambers were cleaned with a 3% vinegar solution to remove trace chemicals from vaporized e-liquids.

Mice were used in the same EVSA paradigm regardless of age (adolescent and adults). Mice began EVSA on a fixed-ratio 1 (FR1) self-administration schedule on a Monday for 5 daily 2-h sessions, with a weekend abstinence period. Mice were singly placed into air-tight operant chambers. Nosepokes in the active hole of the operant chambers resulted in a 3-s delivery of vaporized e-liquids through the vapor entrance port with a 30-s timeout. During the timeout, a yellow cue-light remained on in the active nosepoke hole. Inactive nosepokes were recorded with no consequences. After session 5, mice were transitioned to a FR2 schedule for 5 sessions and then FR3 for 5 sessions. Next, mice were assigned a progressive ratio (PR) schedule (requiring $n + 1$ nosepokes for each delivery) for 3 sessions and then 2 sessions at FR3. Mean FR3 (sessions 11–15) and PR breakpoint (sessions 16–18) were used as metrics for reinforcement-related behavior and motivation-related behaviors. Similar to our previous EVSA paradigms[8,9,19,22,23], during the first three days of FR1 (sessions 1, 2, and 3), mice were given a non-contingent delivery if they did not nosepoke within specific intervals (8, 12, and 24 min respectively).

Upon completing the EVSA paradigm, mice were euthanized and brains were extracted for physiological or microscopy assays depending on genotype. The only mice sufficient for microscopy assays were those that were positive for both α4-mCherry and α6-GFP as this is necessary for examination of α4α6-containing (α4α6*) nAChRs. Thus, all α4-mCherryα6-GFP mice were used in microscopy assays. Microscopy assays necessitate the rapid freezing of brains; therefore this excludes their use in physiological assays. Mice that were α6-GFP-only or α4-mCherry-only were used in patch-clamp assays for the VTA and mPFC. Slices were collected for VTA or mPFC electrophysiology, and were also obtained for the NAc (for FSCV). These methods are detailed below, it is important to note that the number of mice used in EVSA assays differs from microscopy and physiology assays. For EVSA assays, our adolescent cohorts used 20 females (6 mg/mL nicotine plus menthol), 20 females (60 mg/mL nicotine plus menthol), 16 males (6 mg/mL nicotine plus menthol), 16 males (60 mg/mL nicotine plus menthol), 13 males (PGVG, control), and 12 males (PGVG, control).

Patch-Clamp electrophysiology

EVSA end sessions were staggered so that individual mice could be used for electrophysiological and FSCV assays. Each mouse that completed EVSA assays had brains isolated within 30 min of their final EVSA session. The electrophysiologist was blinded to the conditions of the mice (sex, e-liquid condition, FR3/PR scores), and individual mice were recorded in a randomized order based upon the completion of the EVSA paradigms. Mice were exposed to CO_2 and then a cardiac perfusion was performed using ice-cold NMDG-based artificial cerebrospinal fluid (NMDG-ACSF) saturated with 95%/5% O_2/CO_2 (carbogen) containing (in mM): 93 NMDG, 2.5 KCl, 1.2 NaH_2PO_4, 10 $MgSO_4$, 0.4 $CaCl_2$, 30 $NaHCO_3$, 5 Na-ascorbate, 3 Na-pyruvate, 2 thiourea, and 25 glucose. Brains were placed in agarose for slicing with a Compresstome® VF-300-OZ (Precisionary Instruments). Coronal brain sections (300 μm) were cut into cold carbogenated NMDG-ACSF to obtain slices containing the mPFC (target bregma +1.8 mm; anterior-posterior limits of +1.7 to +2.3 mm), VTA (target bregma −2.8 to −3.4 mm), and NAc (for FSCV, see below). Slices recovered at 32 °C in carbogenated NMDG-ACSF for 12–15 min. Next, slices were transferred to standard ACSF containing (mM): 125 NaCl, 2.5 KCl, 1.2 NaH_2PO_4, 1.2 $MgCl_2$, 2.4 $CaCl_2$, 26 $NaHCO_3$, and 11 glucose for one hour at 32 °C. One hour later, slices were transferred to the recording chamber and perfused with carbogenated ACSF (1.5–2.0 ml/min) at room temperature.

Neurons were visualized with an Axio Examiner A1 (Zeiss) equipped with an Axiocam 702 mono. Using brain slices from adult/adolescent male/female α4-mCherry mice, we identified putative layer V (LV) pyramidal neurons in the mPFC as these do not contain α4* nAChRs in LV but do in LIV and LVI[20]. We recorded electrophysiological signals with an Integrated Patch-Clamp Amplifier (Sutter) using previously described methods[24,40,41]. Electrodes had resistances of 4 – 10 MΩ when filled with intrapipette solution (in mM): 135 K gluconate, 5 KCl, 5 EGTA, 0.5 $CaCl_2$, 10 HEPES, 2 Mg-ATP, and 0.1 GTP. Recordings were sampled at ≥10 KHz. The junction potential between patch pipette and bath solutions was nulled just before gigaseal formation. Series resistance was monitored without compensation throughout experiments using SutterPatch software and recordings were terminated if series resistance changed by >20%. In whole-cell recordings, recordings were made after 5 min to provide sufficient time for interchange of intrapipette solution with intracellular components.

Intrinsic excitability was assessed by using a stepped current injection protocol in current clamp mode (5 pA steps, −20 pA to 90 pA). Rheobase was determined from the threshold current sufficient to elicit the first action potential. Maximal spiking ability of neurons was tabulated as the maximal action potentials in any of the current steps. Electrophysiological data (Rheobase) was correlated to the mean FR3 active nosepokes from all 5 of the individual mouse's FR3 sessions (FR3 score, sessions 11–15). Resting membrane properties are provided in Table S1.

Fast-scan cyclic voltammetry. At the time of collecting slices for electrophysiology, brain slices containing the NAc were obtained. Thus, slices for FSCV were obtained ~30 min after the conclusion of an individual mouse's EVSA paradigm. As stated above, the EVSA paradigms were staggered so that a single mouse was recorded each day. NAc slices were incubated with mPFC slices and stored in identical conditions. At time of FSCV recordings, slices were placed on a recording stage (on a setup distinct from the electrophysiology setup) and were perfused with carbogenated ACSF at room temperature. Recording and stim electrodes were placed in the NAcc using a 4X or 10X objective. Tonic (5 pulses, 5 Hz) or phasic (5 pulses, 60 Hz) electrical stimulation (350 μA) was triggered with a Master-9 stimulator (AMPI), driven by Demon Voltammetry software. Voltage was swept from −0.4 to 1.2 mV (20 Hz) using a VA-10 voltammeter (NPI electronic GmbH) and controlled with Demon Voltammetry software. Commercial FSCV electrodes were used (CFE-2, NPI electronic GmbH) to interface with the VA-10 headstage. FSCV electrodes were calibrated using 0.1, 1, 10, and 100 μM dopamine standard solutions.

Confocal microscopy. Following EVSA assays, α4-mCherryα6-GFP mice were culled and brains were extracted and quickly frozen on a slurry of dry ice and acetone. Brains were frozen for ≥24 h and then sectioned at 20 μm using a cryostat (Leica CM1950). We collected brain sections that contain the VTA (target bregma, −3.1; AP limits, −3.4 → −2.9). VTA cells were imaged using an Olympus FV3000. Calculations of raw integrated density (RID) were completed using previously established methods[23,41].

Statistics and reproducibility. Experimenters for electrophysiology, FSCV, and confocal assays were blind to experimental conditions. Electrophysiological and confocal correlations were analyzed via simple linear regression. For electrophysiological measurements (rheobase or maximum spikes during current steps), 2–3 cells were recorded for each brain regions for every mouse. Electrophysiological metrics for individual cells were averaged to provide intrinsic excitability metrics for each mouse. For confocal imaging, two independent brain slices were imaged by two distinct experimenters. Values for each brain slice were averaged to provide fluorescence intensity values for each mouse. Additional analysis of self-administration data by linear regression is provided in the supplemental material. Data were determined to follow a non-normal distribution (see individual data points in Figs. 2 and 5). For this reason, we used a nonparametric test (Mann–Whitney U Test). Statistical analyses were conducted using GraphPad Prism. Power analyses were conducted using G*Power (v. 3.1.9.4, See Table S2 for G*Power parameters used for sample size determination).

Reporting summary

Further information on research design is available in the Nature Portfolio Reporting Summary linked to this article.

Data availability

Data supporting the findings within this study are available in Supplementary Information. All source data for graphs are provided in the 'Supplementary Data 1' file. All original data in this study are also available from the corresponding author upon reasonable request. The unique mouse strain used in for this study is available from the Mutant Mouse Resource & Research Centers and are available for general use (MMRRC 068051-MU, https://www.mmrrc.org/catalog/sds.php?mmrrc_id=68051). Mice are also available from the investigator upon request.

Received: 18 May 2024; Accepted: 14 November 2024;
Published online: 21 November 2024

References

1. Birdsey, J. et al. Tobacco product use among U.S. Middle and High School Students - National Youth Tobacco Survey, 2023. *MMWR Morb. Mortal. Wkly Rep.* **72**, 1173–1182 (2023).
2. Parms, T. A. et al. Symptoms of tobacco dependence among middle and high school tobacco users - Data from the 2019-2020 National Youth Tobacco Survey. *Addict. Behav.* **137**, 107537 (2023).
3. Schneller, L. M. et al. Use of Flavored E-Cigarettes and the Type of E-Cigarette Devices Used among Adults and Youth in the US-Results from Wave 3 of the Population Assessment of Tobacco and Health Study (2015-2016). *Int. J. Environ. Res. Public Health* **16**, https://doi.org/10.3390/ijerph16162991 (2019).
4. WHO. WHO Rport on the Global Tobacco Epidemic, 2017. https://apps.who.int/iris/handle/10665/255874 (2017).
5. Soneji, S. S., Knutzen, K. E. & Villanti, A. C. Use of flavored E-Cigarettes among adolescents, young adults, and older adults: findings from the population assessment for tobacco and health study. *Public Health Rep.* **134**, 282–292 (2019).
6. Leventhal, A. M., Tackett, A. P., Whitted, L., Jordt, S. E. & Jabba, S. V. Ice flavours and non-menthol synthetic cooling agents in e-cigarette products: a review. *Tob. Control* https://doi.org/10.1136/tobaccocontrol-2021-057073 (2022).
7. Leventhal, A. M. et al. Flavor and nicotine effects on E-cigarette appeal in young adults: moderation by reason for vaping. *Am. J. Health Behav.* **44**, 732–743 (2020).
8. Cooper, S. Y., Akers, A. T. & Henderson, B. J. Flavors enhance nicotine vapor self-administration in male mice. *Nicotine Tob. Res*. **23**, 566–572 (2021).
9. Henderson, B. J. & Cooper, S. Y. Nicotine formulations impact reinforcement-related behaviors in a mouse model of vapor self-administration. *Drug Alcohol Depend.* **224**, 108732 (2021).
10. Arain, M. et al. Maturation of the adolescent brain. *Neuropsychiatr. Dis. Treat.* **9**, 449–461 (2013).
11. McGlinchey, E. M., James, M. H., Mahler, S. V., Pantazis, C. & Aston-Jones, G. Prelimbic to Accumbens Core pathway is recruited in a dopamine-dependent manner to drive cued reinstatement of cocaine seeking. *J. Neurosci.* **36**, 8700–8711 (2016).
12. Domingo-Rodriguez, L. et al. A specific prelimbic-nucleus accumbens pathway controls resilience versus vulnerability to food addiction. *Nat. Commun.* **11**, 782 (2020).
13. Kim, C. K. et al. Molecular and circuit-dynamical identification of top-down neural mechanisms for restraint of reward seeking. *Cell* **170**, 1013–1027.e1014 (2017).
14. Jobson, C. L. M. et al. Adolescent nicotine exposure induces dysregulation of mesocorticolimbic activity states and depressive and anxiety-like prefrontal cortical molecular phenotypes persisting into adulthood. *Cereb. cortex* **29**, 3140–3153 (2019).
15. Struik, R. F. et al. Dorsomedial prefrontal cortex neurons encode nicotine-cue associations. *Neuropsychopharmacology* **44**, 2011–2021 (2019).
16. Cooper, S. Y. et al. The impact of high or low doses of nicotine in a mouse model of vapor self-administration. *Nicotine Tob. Res.* https://doi.org/10.1093/ntr/ntad136 (2023).
17. Henderson, B. J. et al. Menthol enhances nicotine reward-related behavior by potentiating nicotine-induced changes in nAChR function, nAChR upregulation, and DA neuron excitability. *Neuropsychopharm* https://doi.org/10.1038/npp.2017.72 (2017).
18. Avelar, A. J. et al. Morphine exposure reduces nicotine-induced upregulation of nicotinic receptors and decreases volitional nicotine intake in a mouse model. *Nicotine Tob. Res.* https://doi.org/10.1093/ntr/ntac002 (2022).
19. Henderson, B. J., Richardson, M. R. & Cooper, S. Y. A high-fat diet has sex-specific effects on nicotine vapor self-administration in mice. *Drug Alcohol Depend.* **241**, 109694 (2022).
20. Bloem, B., Poorthuis, R. B. & Mansvelder, H. D. Cholinergic modulation of the medial prefrontal cortex: the role of nicotinic receptors in attention and regulation of neuronal activity. *Front. Neural Circuits* **8**, 17 (2014).
21. Gabbott, P. L., Warner, T. A., Jays, P. R., Salway, P. & Busby, S. J. Prefrontal cortex in the rat: projections to subcortical autonomic, motor, and limbic centers. *J. Comp. Neurol.* **492**, 145–177 (2005).
22. Olszewski, N. A., Tetteh-Quarshie, S. & Henderson, B. J. Neuronal excitability in the medial habenula and ventral tegmental area is differentially modulated by nicotine dosage and menthol in a sex-specific manner. *eNeuro* https://doi.org/10.1523/ENEURO.0380-23.2024 (2024).
23. Cooper, S. Y. et al. Green apple e-cigarette flavorants alter neurobiology in a sex-dependent manner to promote vaping-related behaviors. *J. Neurosci.* **43**, 1360–1374 (2023).
24. Akers, A. T. et al. Upregulation of nAChRs and Changes in Excitability on VTA Dopamine and GABA Neurons Correlates to Changes in Nicotine-Reward-Related Behavior. *eNeuro* **7**, https://doi.org/10.1523/ENEURO.0189-20.2020 (2020).
25. Rice, M. E. & Cragg, S. J. Nicotine amplifies reward-related dopamine signals in striatum. *Nat. Neurosci.* **7**, 583–584 (2004).
26. Nashmi, R. et al. Chronic nicotine cell specifically upregulates functional α4* nicotinic receptors: basis for both tolerance in midbrain and enhanced long-term potentiation in perforant path. *J. Neurosci.* **27**, 8202–8218 (2007).
27. Romoli, B. et al. Neonatal nicotine exposure primes midbrain neurons to a dopaminergic phenotype and increases adult drug consumption. *Biol. Psychiatry* https://doi.org/10.1016/j.biopsych.2019.04.019 (2019).
28. Frie, J. A. et al. Factors influencing JUUL e-cigarette nicotine vapour-induced reward, withdrawal, pharmacokinetics and brain connectivity in rats: sex matters. *Neuropsychopharmacology* https://doi.org/10.1038/s41386-023-01773-3 (2023).
29. Aguilar-Rivera, M. I., Casanova, J. P., Gatica, R. I., Quirk, G. J. & Fuentealba, J. A. Amphetamine sensitization is accompanied by an increase in prelimbic cortex activity. *Neuroscience* **288**, 1–9 (2015).
30. Cass, D. K., Thomases, D. R., Caballero, A. & Tseng, K. Y. Developmental disruption of gamma-aminobutyric acid function in the medial prefrontal cortex by noncontingent cocaine exposure during early adolescence. *Biol. Psychiatry* **74**, 490–501 (2013).
31. de Rover, M. et al. Long-lasting nicotinic modulation of GABAergic synaptic transmission in the rat nucleus accumbens associated with behavioural sensitization to amphetamine. *Eur. J. Neurosci.* **19**, 2859–2870 (2004).
32. Mansvelder, H. D., Keath, J. R. & McGehee, D. S. Synaptic mechanisms underlie nicotine-induced excitability of brain reward areas. *Neuron* **33**, 905–919 (2002).
33. Faure, P., Tolu, S., Valverde, S. & Naude, J. Role of nicotinic acetylcholine receptors in regulating dopamine neuron activity. *Neurosci* **282**, 86–100 (2014).
34. Goldstein, R. Z. & Volkow, N. D. Dysfunction of the prefrontal cortex in addiction: neuroimaging findings and clinical implications. *Nat. Rev. Neurosci.* **12**, 652–669 (2011).
35. Jordan, C. J. & Andersen, S. L. Sensitive periods of substance abuse: early risk for the transition to dependence. *Dev. Cogn. Neurosci.* **25**, 29–44 (2017).
36. Henderson, B. J. & Lester, H. A. Inside-out neuropharmacology of nicotinic drugs. *Neuropharmacology* **96**, 178–193 (2015).
37. Mackey, E. D. et al. α6* nicotinic acetylcholine receptor expression and function in a visual salience circuit. *J. Neurosci.* **32**, 10226–10237 (2012).
38. Xiao, C. et al. Characterizing functional α6β2 nicotinic acetylcholine receptors in vitro: mutant β2 subunits improve membrane expression, and fluorescent proteins reveal responsive cells. *Biochem. Pharm.* **82**, 852–861 (2011).

39. Nashmi, R. et al. Assembly of a4b2 nicotinic acetylcholine receptors assessed with functional fluorescently labeled subunits: effects of localization, trafficking, and nicotine-induced upregulation in clonal mammalian cells and in cultured midbrain neurons. *J. Neurosci.* **23**, 11554–11567 (2003).
40. Avelar, A. J. et al. Why flavored vape products may be attractive: Green apple tobacco flavor elicits reward-related behavior, upregulates nAChRs on VTA dopamine neurons, and alters midbrain dopamine and GABA neuron function. *Neuropharmacology* 107729 https://doi.org/10.1016/j.neuropharm.2019.107729 (2019).
41. Cooper, S. Y., Akers, A. T. & Henderson, B. J. Green apple e-cigarette flavorant farnesene triggers reward-related behavior by promoting high-sensitivity nAChRs in the ventral tegmental area. *eNeuro* https://doi.org/10.1523/eneuro.0172-20.2020 (2020).

Acknowledgements
This work was supported by NIDA (DA050717 to B.J.H.) and NSF (NSF OIA-2242771 support to B.J.H.). Confocal imaging was conducted using equipment in Marshall University's Molecular and Biological Imaging Center (MBIC).

Author contributions
B.J.H. designed the study. Behavior assays were performed by B.J.H., S.T.Q., N.A.O., L.E.Y., M.A.S., M.C.D., M.S.M., S.K.M., S.Y.C., and Z.C.W. Microscopy experiments were performed by L.E.Y, M.A.S., M.C.D., and S.K.M. Electrophysiology was performed by B.J.H. Data was analyzed by B.J.H., S.Y.C., S.K.M., and L.E.Y.

Competing interests
The authors declare no competing interests.

Additional information
Supplementary information The online version contains supplementary material available at https://doi.org/10.1038/s42003-024-07272-5.

Correspondence and requests for materials should be addressed to Brandon J. Henderson.

Peer review information *Communications Biology* thanks Nicholas Graziane and the other, anonymous, reviewer(s) for their contribution to the peer review of this work. Primary Handling Editors: Dr Fereshteh Nugent and Dr Ophelia Bu. A peer review file is available.